Biophysical Journal, Volume *117*

Supplemental Information

How Heterogeneity in Glucokinase and Gap-Junction Coupling Determines the Islet [Ca^{2+}] Response

JaeAnn M. Dwulet, Nurin W.F. Ludin, Robert A. Piscopio, Wolfgang E. Schleicher, Ong Moua, Matthew J. Westacott, and Richard K.P. Benninger

Figure S1: Experimentally demonstrating how heterogeneity in GK activity impact blood glucose and plasma insulin release via gap junction electrical coupling.

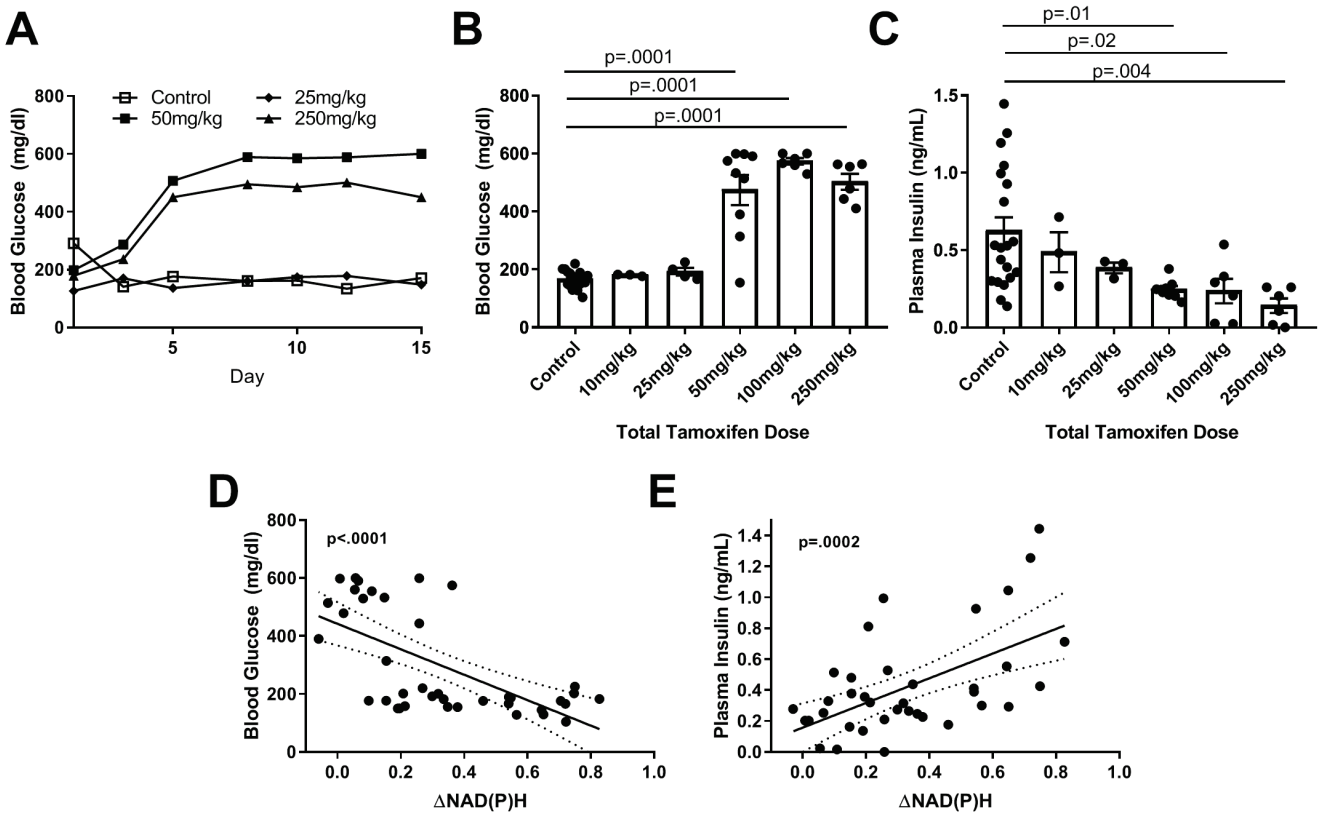

A). Representative time courses for blood glucose measurements for control and 3 tamoxifen doses used for mice with $Cx36^{+/+}$. B). Final blood glucose measurements before isolation vs. tamoxifen dose. C). Plasma insulin on day of isolation vs. tamoxifen dose. D). Linear regression of blood glucose vs. change in NAD(P)H (solid line) with 95% CI (dashed). E). Linear regression line of mice plasma insulin values vs. change in NAD(P)H, as in D. For blood glucose: for control n=19, for 10mg/kg n=3, for 25 mg/kg n=4, for 50mg/kg n=9, for 100mg/kg n=6, for 250mg/kg n=6. For plasma insulin control n=20, for 10mg/kg n=3, for 25 mg/kg n=3, for 50mg/kg n=8, for 100mg/kg n=6, for 250mg/kg n=6. For ΔNADH regression, n=39 for blood glucose and n=38 for plasma insulin.

Figure S2: Simulations predicting how heterogeneity in metabolic activity, with uniform K_{ATP} activity, impacts islet function.

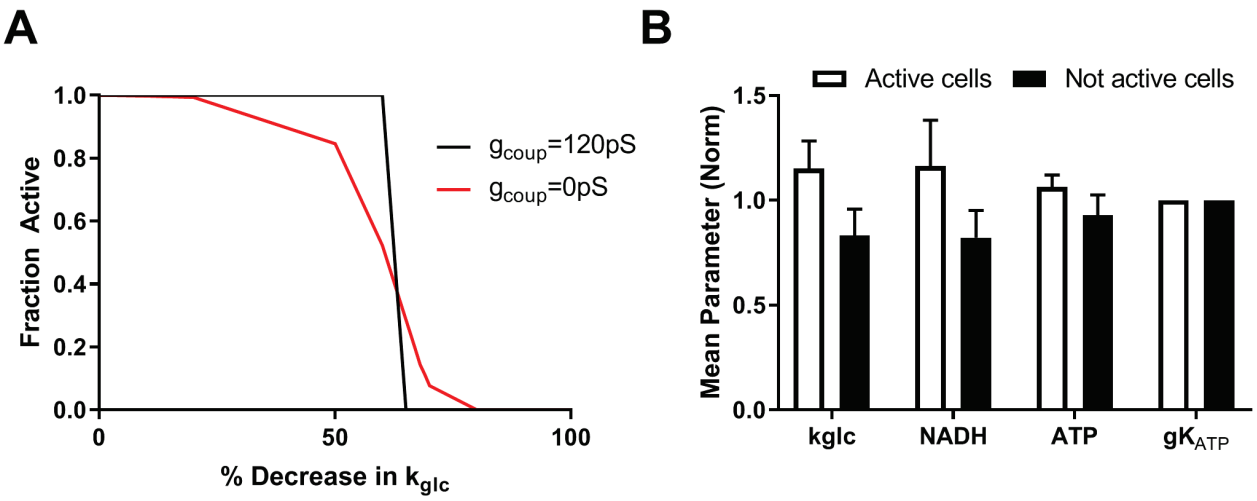

A). Fraction of cells showing elevated [Ca^{2+}] activity ('active cells') in a representative simulated islet that excludes heterogeneity in g_{KATP}, vs. fractional decrease in k_{glc} (decreasing GK activity) for g_{coup} = 120pS and 0pS. B). Average parameter values in [Ca^{2+}] active cells and non-active cells within a simulated islet with g_{coup}=0pS and 60% decrease in k_{glc}. Data in B. represents mean ± SD across all active or inactive cells.

Figure S3: Simulations predicting how other factors underlying GK kinetics impact islet function.

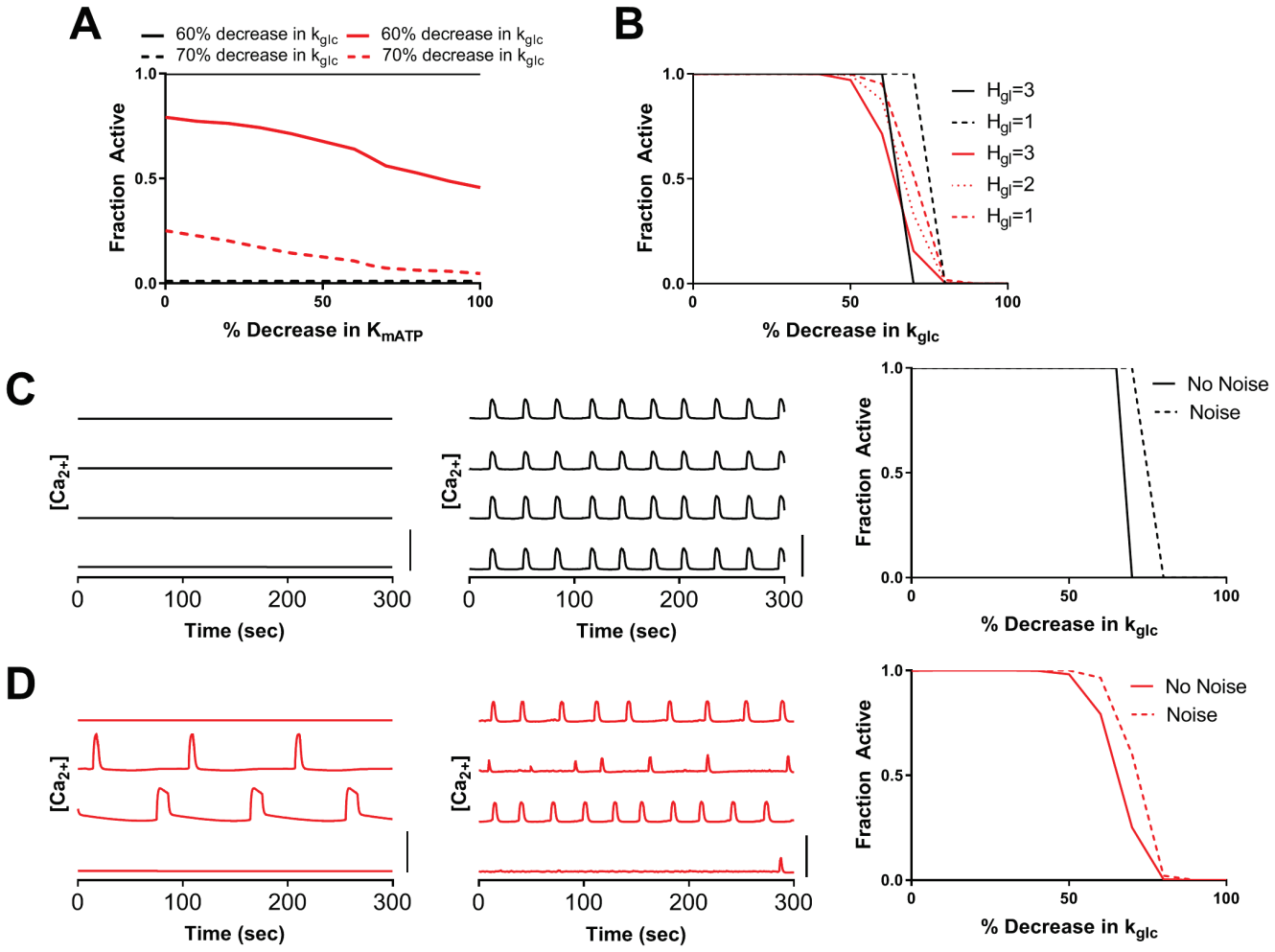

A). Fraction of active cells vs. decreases in the half maximal concentration of ATP (K_{mATP}), with g_{coup}=120pS (black) and g_{coup}=0pS (red), each for two different values of k_{glc} (higher k_{glc} solid, lower k_{glc} dashed). B). Fraction of active cells for several different hill coefficients for the glucose dependence of GK activity, with g_{coup}=120pS and g_{coup}=0pS. C). $[Ca^{2+}]$ activity with and without stochastic noise present in the model. Left: Representative time courses for 4 individual cells with g_{coup}=120pS without stochastic noise at 70% decrease in k_{glc}. Middle: Representative time courses for 4 individual cells in simulations with stochastic noise at 65% decrease in k_{glc}. Right: Fraction of active cells for simulations with and without noise vs. % decrease in k_{glc}. D). As in C. but for simulations with g_{coup}=0pS. Scale bar in C,D represents 0.5μM.

Figure S4: All simulation data from MODY-2 mutations.

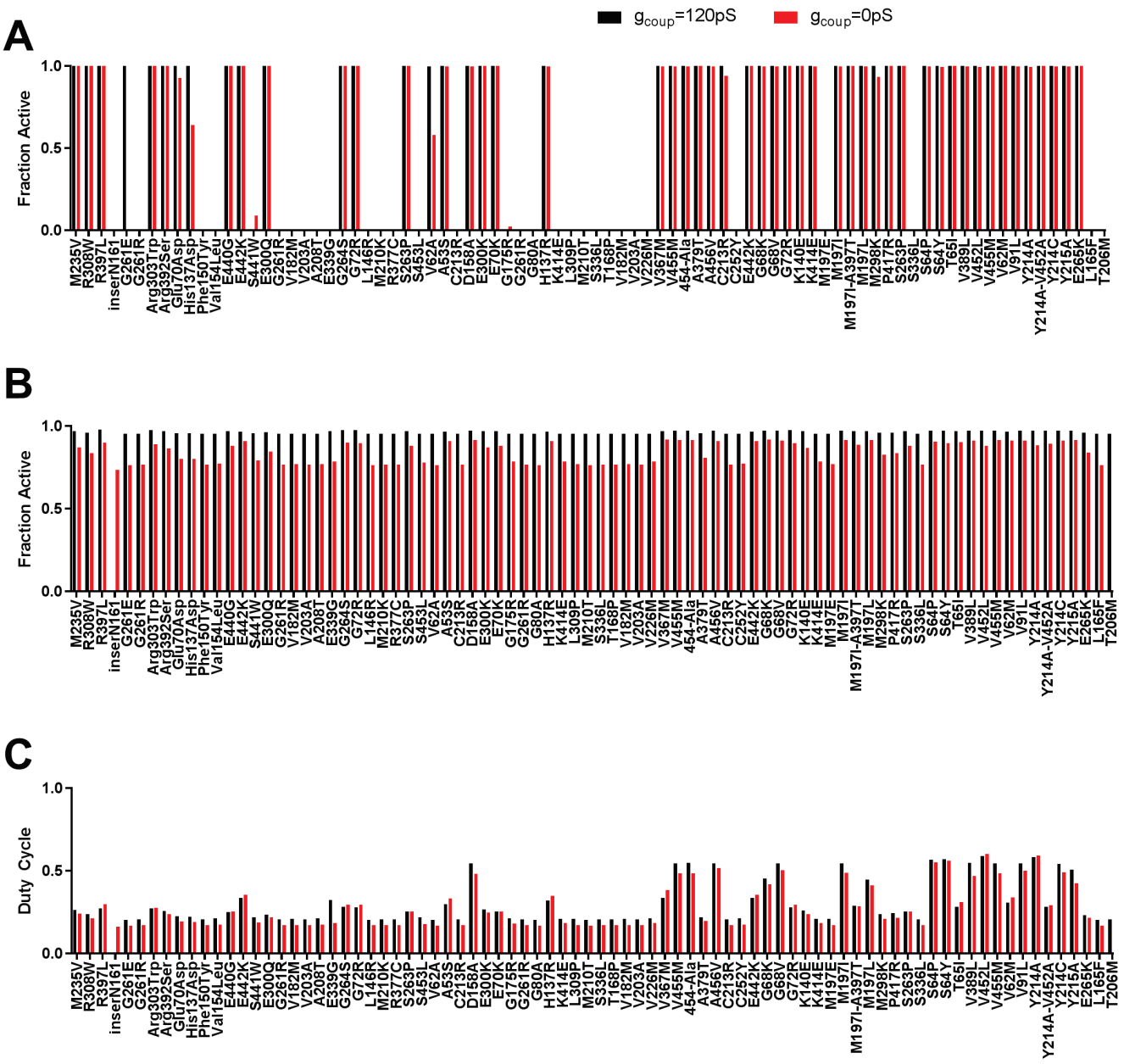

A). Fraction of active cells from all MODY-2 mutations used with homozygous GK activity at 20mM glucose. B). Fraction of active cells from all MODY-2 mutations used with heterozygous GK activity at 11mM glucose. C). Average duty cycle for all MODY-2 mutations used with heterozygous GK activity at 11mM glucose. Black bars are simulations with g_{coup} = 120pS and red bars are g_{coup}=0pS, n=82 simulations.

Figure S5: Simulations predicting how heterozygous expression of human MODY-2 GK impacts islet function.

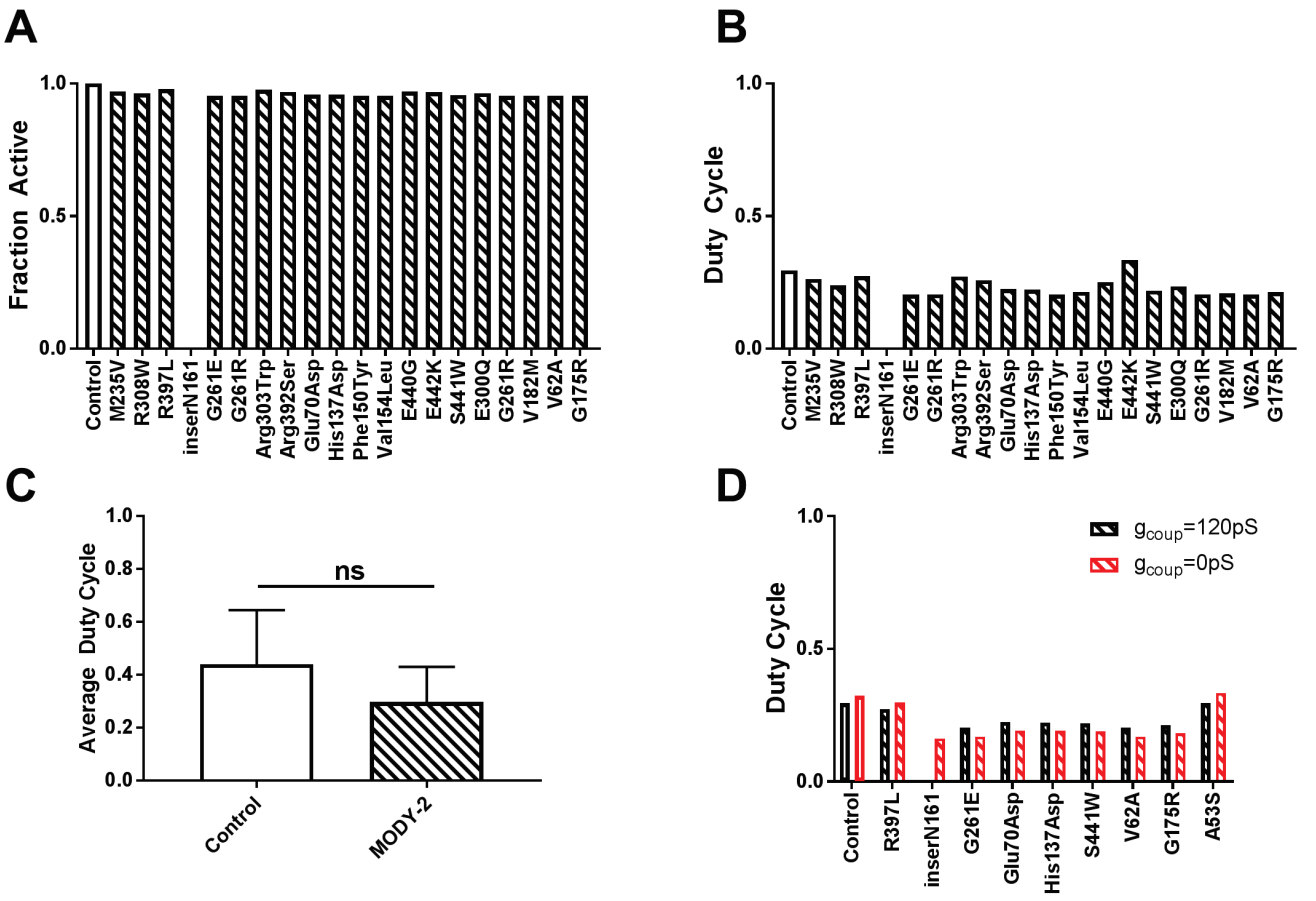

A). Fraction of active cells for representative simulations of human MODY-2 mutations that were simulated as heterozygous GK activity (See Methods) at 11mM glucose. Mutations are those representative ones presented in Figure 6b. B). Duty cycle for heterozygous mutations for MODY-2 compared with control simulation (as in A and in Figure 6b) at 11mM glucose. C). Average duty cycle for all mutations (n=82) and all control simulations (n=2) at 11mM glucose. D). Representative results for duty cycle from heterozygous simulations for g_{coup}=120pS and g_{coup}=0pS. Mutations are those representative ones presented in Figure 6g. Data in C,D presented as mean±SD.

Figure S6: Simulations categorized by HbA1c severity.

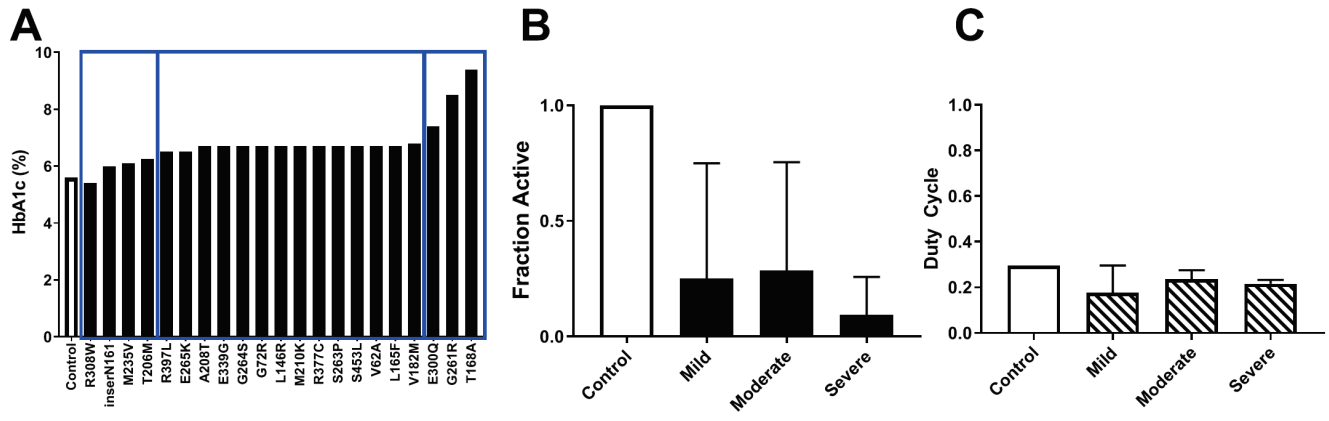

A). HbA1c with bins chosen (blue rectangles) for mild, moderate, and severe mutations, ordered from left to right. B). Mean fraction of active cells from simulations of mutations in A. at 11mM glucose, averaging over the disease severity and considering homozygous mutations. C). Average duty cycle for mutations in A at 11mM glucose averaging over the disease severity and considering heterozygous mutations. All simulations run with g_{coup}=120pS. Data in B and C represent mean±SD.

Figure S7: Summarizing computational and experimental results in the presence of GK heterogeneity.

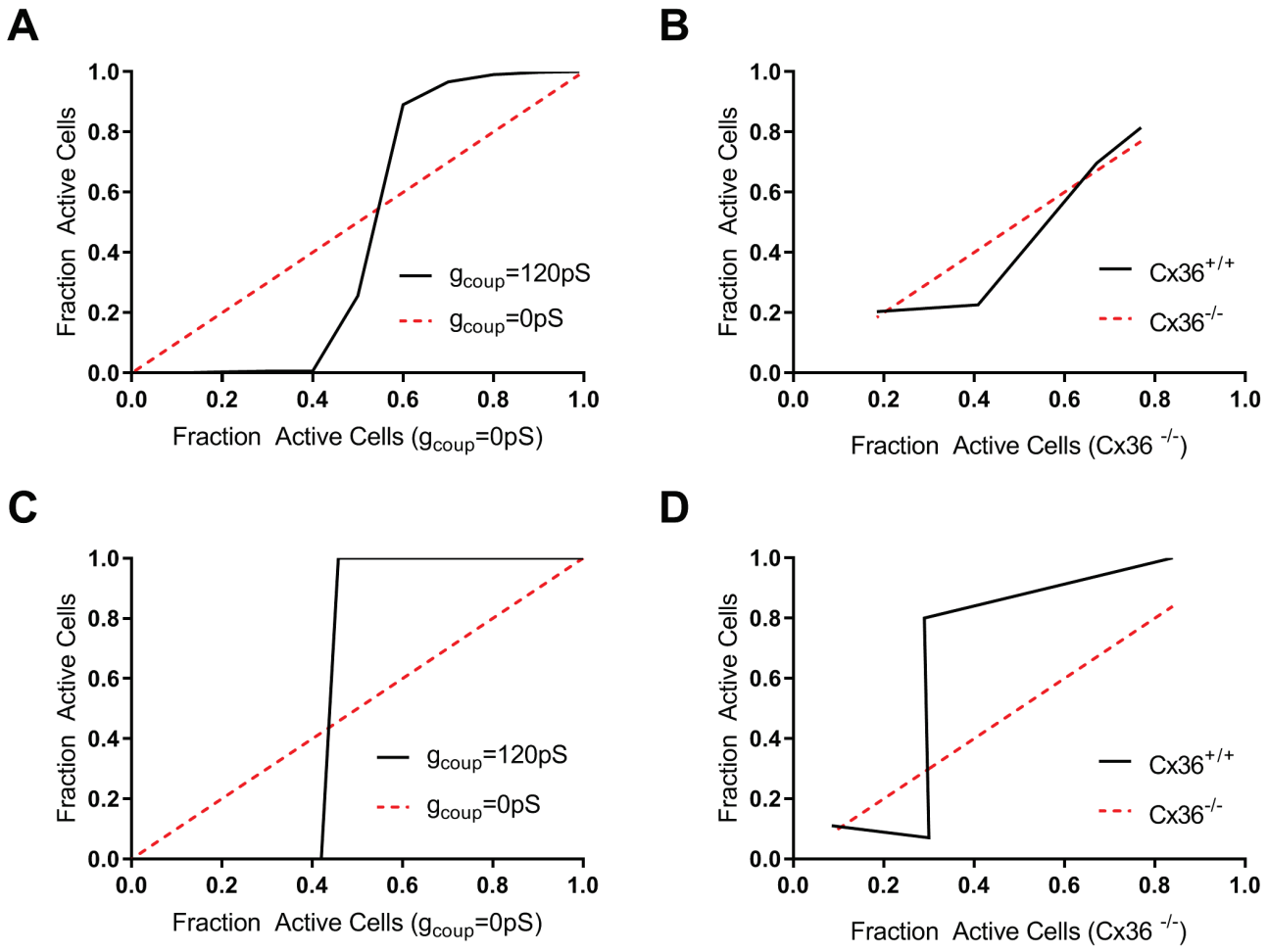

A). Simulations demonstrating the transition from islet-wide elevated $[Ca^{2+}]$ to complete suppression in islets with varying proportion of cells that are unable to respond to $[Ca^{2+}]$, in this case because of deficiency in GK (GK-). Plotted is data from figure 1 with defined populations of GK deficient cells, displaying the proportion of cells showing elevated $[Ca^{2+}]$ in the absence of gap junction electrical coupling against in the presence of gap junction electrical coupling. B) As in A for experimental measurements plotting data from figure 2 with defined populations of GK deficient cells. C) As in A for simulations plotting data from figure 3 with continuous distribution of GK activity. D) As in A for experimental measurements plotting data from figure 4 with the endogenous distribution of GK activity. For islets with zero gap junction electrical coupling the transition is trivially linear (red dashed).

Table S1: List of GCK mutations simulated in this study.

PNDM *GCK* mutations								
Number	**Mutation**	**k_glc (s-1)**	**K_G mM**	**Km_ATP (mM)**	**Hill (unitless)**	**OGTT (mg/dl)**	**HbA1c (%)**	**Citation**
1	A378V	55.4	576	9.92	0.94			55
2	G264S	63.5	9.76	0.48	1.57			55
	Control	64.2	7.56	0.37	1.77			55
3	T168A	5.33	25.47	7.89	0.86			52
	Control	61.52	7.39	0.64	1.58			53
4	M210K	16.7	38.7	1.38	1.63			36
5	T228M	0.004	5.5	0.62	0.71			36
	Control	52.4	7.7	0.35	1.66			36

MODY-2 *GCK* mutations								
Number	**Mutation**	**k_glc (s-1)**	**K_G mM**	**Km_ATP (mM)**	**Hill (unitless)**	**OGTT (mg/dl)**	**HbA1c (%)**	**Citation**
1	M235V	22.9	7.8	0.46	1.38	147.6	6.1	51
2	R308W	22.3	10.7	0.5	1.36	226.8	5.4	51
3	R397L	42.1	7.7	0.46	1.5	154.8	6.5	51
4	inserN161	0.29	155	0.32	0.99	198	6	51
	Control	55.5	7.6	0.49	1.42			51
5	G261E	3.72	334.73	2.99	1.92			50
6	G261R	17.03	68.61	0.63	1.53			50
	Control	62.3	7.55	0.41	1.74			50
7	Arg303Trp	14.6	4.62	0.29	1.52			49
8	Arg392Ser	41.3	11.9	0.63	1.3			49
9	Glu70Asp	27.4	20.1	0.25	1.2			49
10	His137Asp	17.2	18.1	0.23	1.1			49
11	Phe150Tyr	9.92	101.4	3.11	1.06			49
12	Val154Leu	46.6	26	1.62	1.54			49
	Control	44.1	7.2	0.4	1.4			49
13	E440G	51.55	10.85	0.74	1.52	108.9	N/A	48
14	E442K	41.98	4.43	0.72	1.6	N/A	N/A	48
15	S441W	20.72	15.89	1.12	1.38	144.9	N/A	48
	Control	65.57	7.97	0.45	1.71			48
16	E300Q	100	20			122.4	7.4	56
17	G261R	0.46	2.5			207	8.5	56
18	V182M	49	70			223.2	6.8	56
19	V203A	0.5	100			102.6	N/A	56
	Control	100	8			95.4	N/A	56
20	A208T	4.41	10.1	2.61	1.23	171*	6.7*	47
21	E339G	60.2	32.1	1.87	1.34	171*	6.7*	47
22	G264S	65.3	9.76	0.48	1.57	171*	6.7*	47
23	G72R	33.5	5.32	0.76	1.45	171*	6.7*	47
24	L146R	0.21	123	0.1	0.95	171*	6.7*	47
25	M210K	26.7	52.8	1.58	1.64	171*	6.7*	47
26	R377C	5.92	52.3	0.28	1.64	171*	6.7*	47
27	S263P	64.7	12.2	0.51	1.59	171*	6.7*	47
28	S453L	8.89	16	0.69	1.39	171*	6.7*	47
29	V62A	39	24.6	0.2	1.5	171*	6.7*	47
	Control	63	7.55	1.74	0.41	91.8	5.6	47
30	A53S	45.2	8.1	0.22	1.8			45
31	C213R	14.1	58.4	0.85	1.76			45
32	D158A	52.2	3.67	0.33	1.7			45
33	E300K	33.8	10.3	0.46	1.85			45
34	E70K	43.2	11.5	0.36	1.78			45
35	G175R	17.1	19.6	0.45	1.74			45

36	G261R	1.04	118	3.83	2.2			45
37	G80A	0.06	965	7.71	0.64			45
38	H137R	44.7	7.46	0.24	1.8			45
39	K414E	11	12.3	1.73	1.67			45
40	L309P	1.1	9.46	0.58	1.92			45
41	M210T	6.22	234	5.68	1.36			45
42	S336L	1.03	5.42	21.7	1.13			45
43	T168P	0.35	160	9.33	0.92			45
44	V182M	12.2	34.9	0.11	1.7			45
45	V203A	12.3	58.4	0.88	1.53			45
46	V226M	42.7	17.9	5.74	1.41			45
47	V367M	58.1	7.56	0.31	1.8			45
48	V455M	48.6	3.18	0.25	1.66			45
	Control	51.5	8.33	0.31	1.8			45
49	454-Ala	52.2	1.38	0.31	1.62			57
50	A379T	61.2	12.3	0.87	1.6			57
51	A456V	65.6	1.91	0.35	1.37			57
52	C213R	50	21.6	0.89	1.43			57
53	C252Y	29.3	31.6	0.75	1.54			57
54	E442K	52.6	5.24	1.5	1.72			57
55	G68K	43.2	2.34	0.39	1.33			57
56	G68V	62.7	2.2	0.31	1.35			57
57	G72R	29.8	7.38	0.72	1.42			57
58	K140E	40	10.8	0.35	1.57			57
59	K414E	19.9	5.69	1.53	1.52			57
60	M197E	17.7	41.6	0.4	1.4			57
61	M197I	58.1	2.49	1.39	1.8			57
62	M197I-A397T	50.2	5.81	2.71	1.36			57
63	M197L	62.6	4.03	1.31	1.6			57
64	M298K	37.7	10.8	3.32	1.28			57
65	P417R	48.3	6.59	2.08	1.52			57
66	S263P	44.6	9.7	0.63	1.66			57
67	S336L	2.46	4.75	12.6	0.95			57
68	S64P	83.3	2.07	0.32	1.31			57
69	S64Y	114	1.89	1.59	1.5			57
70	T65I	22.6	1.69	0.57	1.3			57
71	V389L	67.1	3.45	0.76	1.54			57
72	V452L	122	2.27	0.53	1.46			57
73	V455M	61.8	3.24	0.38	1.62			57
74	V62M	47.2	5.9	0.52	1.38			57
75	V91L	60.6	1.66	0.48	1.42			57
76	Y214A	117	1.41	0.92	1.41			57
77	Y214A-V452A	23.1	0.55	1.42	0.88			57
78	Y214C	65.3	1.35	1.08	1.55			57
79	Y215A	44.7	2.07	0.58	1.46			57
	Control	62.8	7.45	0.46	1.77			57
80	E265K	36.8	15.5	0.63	1.43	N/A	6.5	58
81	L165F	18	92.5	1.52	1.21	205.2	6.7	58
82	T206M	0.18	85	0.45	0.9	167.4	6.25	58
	Control	42	8	0.4	1.53			58

Mutations separated by PNDM and MODY2. Number represents order of appearance in Figure 6 or S4 Figure. Control represents wild-type GK. N/A indicates data not available. * indicates average value in cited study (individuals not presented).

File S1: Model code used in this study.

(see accompanying zip file)